

The R3 receptor-like protein tyrosine phosphatase subfamily inhibits insulin signalling by dephosphorylating the insulin receptor at specific sites

Received March 13, 2015; accepted March 19, 2015

Takafumi Shintani^{1,2}, Satoru Higashi^{1,2},
Yasushi Takeuchi¹, Eugenio Gaudio^{3,*},
Francesco Trapasso³, Alfredo Fusco⁴ and
Masaharu Noda^{1,2,†}

¹Division of Molecular Neurobiology, Department of Neurobiology, National Institute for Basic Biology, Okazaki 444-8787, Japan; ²Department of Basic Biology, School of Life Science, The Graduate University for Advanced Studies (SOKENDAI), Okazaki 444-8787, Japan; ³Dipartimento di Medicina Sperimentale e Clinica, University Magna Graecia, Campus “S. Venuta”, Catanzaro 88100, Italy; and ⁴Istituto di Endocrinologia ed Oncologia Sperimentale del CNR c/o Dipartimento di Medicina Molecolare e Biotecnologie Mediche, Scuola di Medicina e Chirurgia di Napoli, Università degli Studi di Napoli Federico II, Napoli 80138, Italy

*Present address: Eugenio Gaudio, Lymphoma and Genomics Research Program, IOR Institute of Oncology Research, Bellinzona 6500, Switzerland

†Masaharu Noda, Division of Molecular Neurobiology, National Institute for Basic Biology, Okazaki 444-8787, Japan. Tel: +81-564-59-5846, Fax: +81-564-59-5845, email: madon@nibb.ac.jp

The autophosphorylation of specific tyrosine residues occurs in the cytoplasmic region of the insulin receptor (IR) upon insulin binding, and this in turn initiates signal transduction. The R3 subfamily (Ptp^{rb}, Ptp^{rh}, Ptp^{rj} and Ptp^{ro}) of receptor-like protein tyrosine phosphatases (RPTPs) is characterized by an extracellular region with 6–17 fibronectin type III-like repeats and a cytoplasmic region with a single phosphatase domain. We herein identified the IR as a substrate for R3 RPTPs by using the substrate-trapping mutants of R3 RPTPs. The co-expression of R3 RPTPs with the IR in HEK293T cells suppressed insulin-induced tyrosine phosphorylation of the IR. *In vitro* assays using synthetic phosphopeptides revealed that R3 RPTPs preferentially dephosphorylated a particular phosphorylation site of the IR: Y960 in the juxtamembrane region and Y1146 in the activation loop. Among four R3 members, only Ptp^{rj} was co-expressed with the IR in major insulin target tissues, such as the skeletal muscle, liver and adipose tissue. Importantly, the activation of IR and Akt by insulin was enhanced, and glucose and insulin tolerance was improved in Ptp^{rj}-deficient mice. These results demonstrated Ptp^{rj} as a physiological enzyme that attenuates insulin signalling *in vivo*, and indicate that an inhibitor of Ptp^{rj} may be an insulin-sensitizing agent.

Keywords: diabetes/insulin receptor/insulin signalling/protein tyrosine phosphatase/Ptp^{rj}-deficient mice.

Abbreviations: CNS, central nervous system; ICR, intracellular region; IR, insulin receptor; IRS, insulin receptor substrate; PTK, protein tyrosine kinase;

PTP, protein tyrosine phosphatase; PTP-1B, protein tyrosine phosphatase 1B; Ptp^{rb}, protein tyrosine phosphatase receptor type B; Ptp^{rh}, protein tyrosine phosphatase receptor type H; Ptp^{rj}, protein tyrosine phosphatase receptor type J; RPTK, receptor PTK; RPTP, receptor-like PTP.

Insulin, which is secreted by β cells in the pancreatic islets of Langerhans in response to an increase in blood glucose levels, plays a central role in regulating energy metabolism including glucose and lipid metabolism (1, 2). Insulin signalling is initiated when insulin binds to the insulin receptor (IR), a member of the receptor protein tyrosine kinase (RPTK) superfamily, on the surface of target cells such as skeletal muscle, liver and adipose cells. When insulin binds to the IR, it is activated by autophosphorylation and subsequently phosphorylates tyrosine residues on insulin receptor substrates (IRSs) bound to the IR. This stimulates the recruitment of SH2 domain proteins including phosphatidylinositol 3-kinase to IRSs, and activates downstream signalling pathways (1, 2). Insulin signalling is integral to the regulation of glucose homeostasis in the liver, striated muscle and adipose tissue because it promotes glucose uptake and glycogen synthesis and inhibits glycogenolysis and gluconeogenesis (1, 2). Insulin resistance in these tissues, which has been attributed to defects in IR signalling, is the underlying pathogenic feature of type 2 diabetes (1).

Reversible tyrosine phosphorylation is an important mechanism for the regulation of variegated cellular functions. The tyrosine phosphorylation levels of a cellular protein are determined by the balance between the activities of specific protein tyrosine kinases (PTKs) and protein tyrosine phosphatases (PTPs). PTPs are therefore considered to be central players that regulate insulin signalling by opposing the activity of PTKs (3, 4). Extensive efforts have been undertaken to identify PTPs that negatively regulate IR activity (5–10). Among the candidate PTPs identified to date, protein tyrosine phosphatase 1B (PTP-1B) has been examined the most extensively. PTP-1B is a non-receptor-type PTP that is attached to the cytoplasmic face of the endoplasmic reticulum (ER) (11). It is ubiquitously expressed in the body and is known to control a multitude of signalling events during cell growth, differentiation, apoptosis and cell movement (12, 13). PTP-1B

preferentially dephosphorylates tyrosine residues at 1150 and 1151 (the amino acid residue number in mouse IR) in the activation loop of the IR, which leads to inactivation of the IR (14). *PTP-1B*-deficient mice exhibit increased systemic insulin sensitivity, improved glucose tolerance and enhanced liver IR phosphorylation (15, 16). Thus, PTP-1B is a physiological negative regulator of insulin signalling; however, the contribution of other PTPs to the regulation of insulin signalling remains unclear.

The human genome encodes 107 PTPs (17), 38 of which are classical tyrosine-specific PTPs. Of these, 20 members are transmembrane receptor-like PTPs (RPTPs), while 18 members are intracellular PTPs. RPTPs consist of an extracellular region, single transmembrane segment and cytoplasmic region with one or two tyrosine phosphatase domains. RPTPs have been classified into eight subfamilies (R1/R6, R2a, R2b, R3, R4, R5, R7 and R8) based on the sequence homologies of their extracellular and PTP domains (18). We previously performed large-scale screening of the enzyme–substrate relationship between the R3 RPTPs (Ptp_{rb}, Ptp_{rh}, Ptp_{rj} and Ptp_{ro}) and RPTKs using mammalian two-hybrid assays with substrate-trapping RPTP mutants (19). The R3 RPTP subfamily is characterized by the extracellular region, composed of fibronectin type III-like repeats, and the intracellular region (ICR), containing a single phosphatase domain (18). We identified multiple RPTKs as substrates for R3 subfamily members (19).

We continued screening, and herein reported that the IR was a substrate for the R3 subfamily. The co-expression of R3 RPTPs with the IR in HEK293 suppressed activation of the IR. Synthetic peptide-based assays revealed that R3 RPTPs preferentially dephosphorylated particular phosphorylation sites of the IR: Y960 in the juxtamembrane region and Y1146 in the activation loop. Among R3 RPTPs, Ptp_{rj} was found to be expressed with the IR in insulin target tissues including the skeletal muscle, liver and adipose tissue. In HEK293T cells, Ptp_{rj} was co-localized with the IR at the subcellular level. In line with these results, *Ptp_{rj}*-deficient mice showed enhanced insulin signalling; an enhancement in the insulin-induced activation of the IR and Akt in the liver, and improved glucose and insulin tolerance.

Materials and Methods

Antibodies

Anti-Myc and anti-hemagglutinin (HA) antibodies were purchased from Sigma-Aldrich. An anti-phosphotyrosine antibody (4G10) was from Merck Millipore. Anti-Akt and anti-phosphorylated Akt (S473) antibodies were from Cell Signaling Technologies. An anti-IR antibody was from Santa Cruz. Horseradish peroxidase (HRP)-conjugated and Alexa-conjugated secondary antibodies were from Life Technologies.

DNA constructs

Mouse *IR* complementary DNA (cDNA) was cloned by reverse transcription polymerase chain reaction (RT-PCR) using total RNA from the mouse brain. The ICRs of mouse IR was subcloned into a pCMV-BD-vector (Stratagene) to produce fusion proteins comprising the Gal4 DNA-binding domain and RPTK ICR (BD-RPTKs). The full-length cDNA of the mouse IR was subcloned into the expression vector pcDNA-Myc to produce a Myc-tagged IR protein (IR-Myc). RPTP constructs were described previously (19).

Mammalian two-hybrid assay

Mammalian two-hybrid assays were performed as described (19).

Cell culture and transfection

HEK293T cells were grown in Dulbecco's Modified Eagle's Medium (DMEM)/F-12 medium (1:1, Nissui, Tokyo, Japan) supplemented with 10% foetal bovine serum. Transfection was performed using LipofectAMINE PLUS (Life Technologies) according to the manufacturer's protocol.

Immunoblotting

Cells were lysed in a lysis buffer, which consisted of 20 mM Hepes, pH 7.4, 120 mM NaCl, 0.1% sodium dodecyl sulfate (SDS), 0.5% deoxycholate, 1% Nonidet P-40, 10% glycerol, 5 mM ethylenediaminetetraacetic acid (EDTA), 50 mM NaF, 0.5 mM Na₃VO₄ and a protease inhibitor mixture (10 µg/ml leupeptin, 1 µg/ml pepstatin A and 1 mM phenylmethylsulfonyl fluoride). Cell lysates were clarified by centrifugation, and protein concentrations were determined using the BCA microassay kit (Life Technologies). The extracts were combined with SDS sample buffer and treated for 15 min at 75°C. Ten micrograms of each sample was then subjected to SDS-polyacrylamide gel electrophoresis (PAGE). Separated proteins were transferred onto Immobilon-P membranes (Merck Millipore), incubated with specific primary antibodies and peroxidase-linked secondary antibodies (GE Healthcare), followed by detection with chemiluminescence using ECL Reagent (GE Healthcare). The lumino-image analyzer LAS-3000 (Fujifilm, Japan) was used for this detection. Signal intensity was quantified by densitometry.

In vitro dephosphorylation assay

Glutathione S-transferase (GST) fusion proteins encoding the entire ICRs of R3 RPTPs were described previously (19). Regarding *in vitro* dephosphorylation, we first prepared autophosphorylated IR proteins as the substrate. HEK293T cells expressing Myc-tagged IR were treated with 50 ng/ml insulin for 15 min, and IR proteins were purified by immunoprecipitation with an anti-Myc antibody and protein G-Sepharose CL-4B. Protein G beads were washed once and re-suspended in 100 µl of 10 mM Tris-HCl, pH 7.0, containing 5 mM dithiothreitol, 5 mM EDTA and 100 µg/ml bovine serum albumin (BSA) (protein tyrosine phosphatase (PTP) buffer). In the dephosphorylation assay, 10 ng of GST-RPTPs or GST alone was reacted with 10 µl of Myc-IR at 30°C. At the indicated time, the reaction was stopped by the addition of SDS sample buffer. Samples were separated by SDS-PAGE followed by immunoblotting with an anti-phosphotyrosine antibody.

Phosphatase assay with phosphopeptides

Phosphatase assays were performed as described (20).

Reverse transcription polymerase chain reaction

Total RNA was extracted using Trizol reagent (Life Technologies) following the manufacturer's instructions. Total RNAs were reverse transcribed using SuperScript II reverse transcriptase (Life Technologies). cDNAs were amplified using Ex Taq (Takara) on a T-Professional thermal cycler (Biometa, Germany). The primers were used as follows:

Ptp_{rj}: 5'-TGGAGAAAGAAAAGGACAGATGCCAAGAAT-3' (forward) and 5'-CTAGGCGATGTAACCATTAGTCTTTCCAAAC-3' (reverse); *IR*: 5'-AATGGCAACATCACACACTACC TG-3' (forward) and 5'-AGCTCTGGAAGAAGGGTGATCTC-3' (reverse); *G3p_{dh}*: 5'-ATGGCGTTTCAAAGGCAGTGAAG-3' (forward) and 5'-TCTGCCATCACTGGTTGCAGGATC-3' (reverse). PCR settings were as follows: initial denaturation for 30 s at 95°C was followed by 28 cycles of amplification for 30 s at 95°C and 30 s at 72°C.

In situ hybridization

In situ hybridization was performed as described (21).

Immunocytochemistry

Transfected cells were fixed with 4% paraformaldehyde for 10 min and permeabilized with 0.1% Triton X-100 in phosphate-buffered

saline (PBS) for 5 min. Cells were then incubated for 1 h in a blocking solution (5% BSA in phosphate-buffered saline) at room temperature, and reacted with the primary antibodies for 2 h at room temperature. After washing, cells were treated with the Alexa-conjugated secondary antibody (Life Technologies) at a 1:250 dilution for 30 min at room temperature. The fluorescence signals obtained were observed with a BX51TRF microscope (Olympus, Japan) equipped with a DP-70 digital CCD camera (Olympus, Japan) or Zeiss LSM700 confocal laser microscope (Carl Zeiss), and images were processed using Adobe Photoshop CS3 (Adobe).

Mice

Targeted *Ptprj* heterozygous mice (*Ptprj*^{+/-}) generated in Dr. A. Fusco's laboratory (22) were backcrossed with a C57BL/6 background to give a final five-generation C57BL/6 congenic. After the final backcrossing, *Ptprj*^{+/-} mice were interbred to give littermates for analyses. All sex-matched littermates were co-caged and food and water was provided *ad libitum*. Male mice aged 4 to 6 months were used in this study. Experiments with animals were carried out according to the guidelines of the National Institute for Basic Biology (Okazaki, Japan).

Liver lysate preparation

Livers were dissected from mice, and frozen in liquid N₂, and then ground to a fine powder under liquid N₂. Liver powders were homogenized in ice-cold lysis buffer as described above. Cell lysates were clarified by centrifugation, and protein concentrations were determined using the BCA microassay kit (Life Technologies).

Glucose and insulin tolerance test

In the intraperitoneal glucose tolerance test, mice were injected intraperitoneally with 2 mg/g body weight glucose after overnight fasting. In insulin tolerance test, mice were injected intraperitoneally with insulin (2.0 U/kg) after 6 h of fasting. Blood samples were taken at various time points (0–120 min) from the tail tip, and blood glucose levels were measured with a glucometer (Aventir Biotech, USA).

Results

Identification of the IR as a substrate for the R3 RPTP subfamily by mammalian two-hybrid assays

We exploited mammalian two-hybrid assays with the substrate-trapping DA (Asp → Ala) mutants of PTPs (19, 20) to examine enzyme–substrate interactions between R3 RPTP members (*Ptprb*, *Ptprh*, *Ptprj* and *Ptpro*) and the IR: the DA mutant in which the general aspartic acid (D) residue in the PTP domain was converted to alanine (A) retained the ability to recognize and bind stably to substrates (23). All DA mutants of R3 RPTPs showed specific interactions with the IR (Fig. 1A). In contrast, wild-type (WT) RPTPs did not have the activity to form a stable complex with the IR due to their phosphatase activity (Fig. 1A). These results suggested that R3 RPTPs recognized the IR as their substrate.

We first determined whether *Ptprj* directly dephosphorylated the IR *in vitro* using purified proteins. A Myc-tagged IR was expressed in HEK293T cells, and stimulated with insulin. Autophosphorylated IR proteins were prepared by immunopurification with an anti-Myc antibody. The ICRs of the WT R3 RPTPs were prepared as GST fusion proteins in a similar manner, and were incubated with the IR proteins *in vitro*. All four GST-RPTPs efficiently dephosphorylated the IR (Fig. 1B).

We then investigated whether the full-length R3 RPTPs dephosphorylated the full-length IR in cultured cells. When the IR was expressed alone in HEK293T cells and stimulated with insulin, highly

tyrosyl-phosphorylated IR proteins were detected by an immunoblot analysis (Fig. 1C). The tyrosine phosphorylation levels of the IR were significantly suppressed by the co-expression of R3 RPTPs (Fig. 1C). When the phosphotyrosine levels of the IR were normalized to the expression of each R3 RPTP member, their dephosphorylating activities were judged to be similar among R3 RPTP members (Fig. 1C, right). These results collectively indicated that the IR was a physiological substrate for the R3 RPTP subfamily.

Identification of specific dephosphorylation sites in the IR by R3 RPTP members

When insulin binds to the IR, it is autophosphorylated at several tyrosine residues; the major sites are Y960, Y1146, Y1150, Y1151, Y1316 and Y1322 (Fig. 2A) (24). The autophosphorylation of Y1146, Y1150 and Y1151 in the activation loop is known to be required for maximal activation (1, 25), while the phosphorylation of other sites regulates interactions with signalling molecules (1).

We attempted to identify the tyrosine residues in the IR that are dephosphorylated by R3 RPTPs. To achieve this, we performed an *in vitro* phosphatase assay using synthetic phosphopeptides corresponding to the mouse IR sequence (Fig. 2B). All R3 RPTP members preferentially dephosphorylated the peptides containing phosphorylated Y960 and Y1146 (Fig. 2C). These results indicated that R3 RPTPs preferentially dephosphorylated Y960 in the juxtamembrane region and Y1146 in the activation loop of the IR.

Co-expression of *Ptprj* with the IR in insulin target tissues and co-localization of *Ptprj* proteins with the IR in HEK293T cells

Ptprj is known to be broadly expressed in various tissues (26), while the expression of *Ptprb*, *Ptprh* and *Ptpro* was shown to be restricted in endothelial cells, the intestine and the brain and kidney, respectively (27–29). Therefore, we considered *Ptprj* to be the physiological counterpart, and thus, examined it in more detail. RT-PCR analyses revealed that *Ptprj* was expressed in insulin target tissues; the skeletal muscle, liver and adipose tissue (Fig. 3A). *In situ* hybridization reconfirmed the expression of *Ptprj* in these tissues (Fig. 3B).

We next examined the subcellular distribution of *Ptprj* and IR proteins in HEK293T cells, and found that *Ptprj* co-localized with the IR at the cell surface before and after the insulin stimulation (Fig. 3C, data not shown). These results suggested that *Ptprj* played an important role in glucose metabolism through dephosphorylation of the IR *in vivo*. Therefore, we investigated the effects of a *Ptprj* deficiency on insulin signalling using *Ptprj*-knockout (*Ptprj*-KO) mice.

Enhancement of insulin signalling in *Ptprj*-KO mice

Ptprj-KO mice are viable, fertile and show no gross abnormalities (22). In *Ptprj*-KO mice, insulin signalling was expected to be enhanced due to defects in the dephosphorylation of the IR by *Ptprj*. We first examined activation of the IR in the liver after an

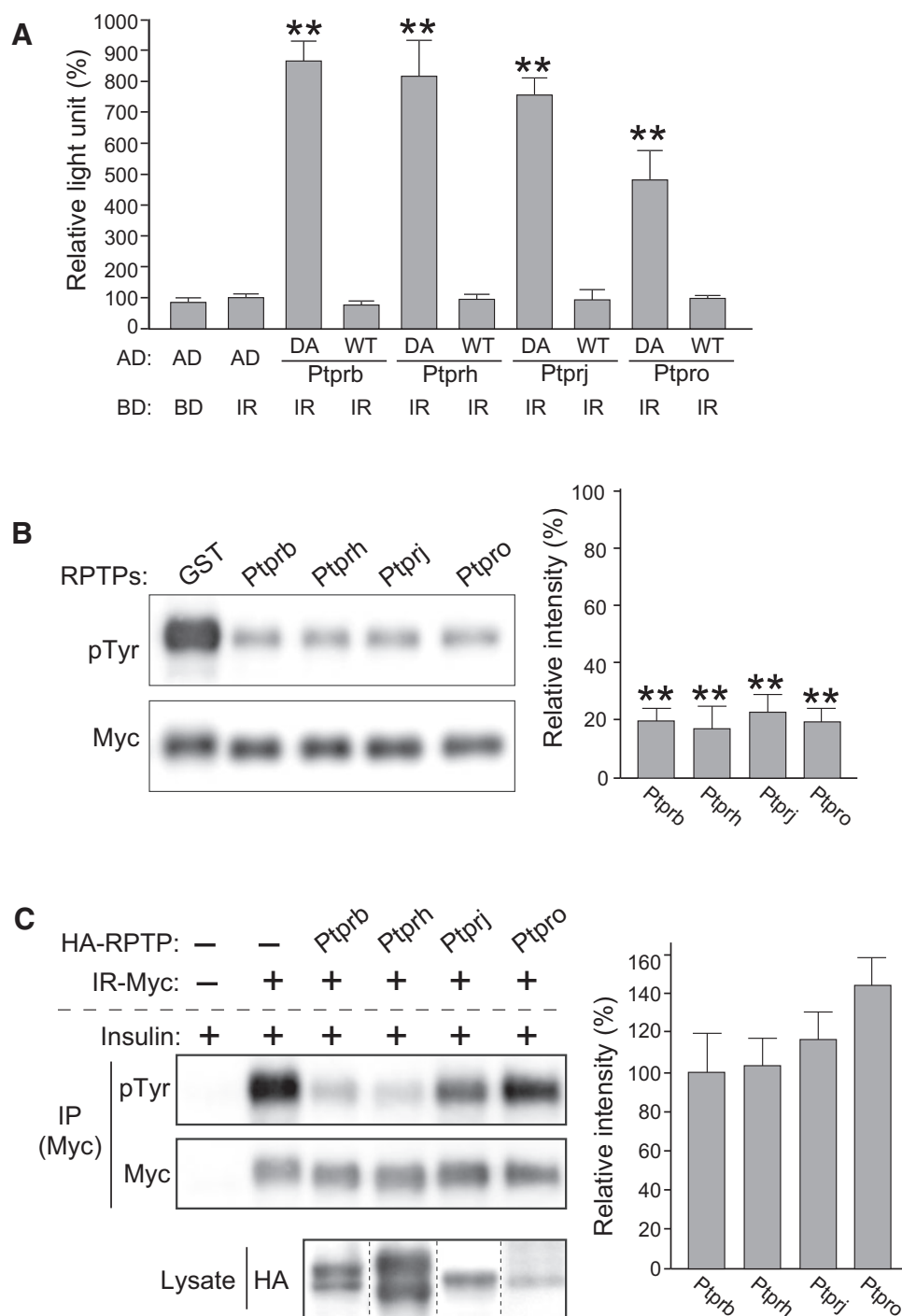


Fig. 1 Identification of the IR as a substrate for the R3 RPTP subfamily. (A) Mammalian two-hybrid analyses to detect interactions between RPTPs and the IR. COS7 cells were transfected with the reporter plasmid pFR-Luc, together with BD-IR and an AD-RPTP expression plasmid. The reporter firefly luciferase value obtained with BD-IR and the empty AD vector (control) was set at 100%, and data obtained with different combinations are shown as relative values. The co-transfected sea pansy luciferase values by pRL-TK were used to normalize the transfection efficacy (19). AD, AD empty vector; BD, BD empty vector; DA, substrate-trapping mutant of RPTPs; WT, wild-type RPTP. Values are shown as the mean \pm SEM ($n = 3$). The asterisk indicates a significant difference from the control by the Student's t -test (** $P < 0.01$). (B) *In vitro* dephosphorylation of the IR by R3 RPTPs. Tyrosine-phosphorylated IR proteins were incubated with an equal amount of GST, GST-Ptprb, GST-Ptprh, GST-Ptprij or GST-Ptpro. After the reaction, proteins were separated by SDS-PAGE and subjected to immunoblotting using an anti-phosphotyrosine antibody (pTyr) and anti-Myc antibody (Myc). The right panel shows a summary of the phosphorylation levels of the IR. The phosphorylation levels are relative values to the control level (100%) by the GST protein. Values are shown as the mean \pm SEM ($n = 3$). The asterisk indicates a significant difference from the control by the Student's t -test (** $P < 0.01$). (C) Suppression of tyrosyl phosphorylation of the IR by the co-expression of R3 RPTPs in HEK293T cells. A Myc-tagged IR expression construct was co-transfected with a control empty vector or an expression construct of HA-tagged Ptprb, Ptprh, Ptprij or Ptpro in HEK293T cells. IR proteins were immunoprecipitated with an anti-Myc antibody and analysed with the indicated antibodies by western blotting. RPTP proteins in lysates were detected with an anti-HA antibody. The right panel shows a summary of the phosphorylation level of IR (pTyr). Data were normalized to the Myc level and the average level of expression of RPTPs, and shown as relative values to Ptprb. Values are shown as the mean \pm SEM ($n = 3$).

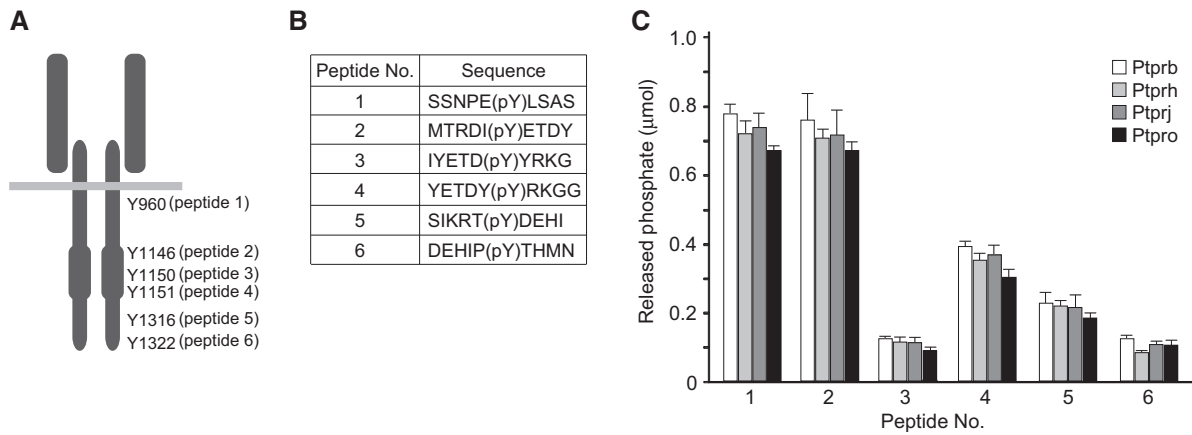


Fig. 2 Phosphatase assays using synthetic phosphopeptides. (A) Schematic representation of autophosphorylation sites in the IR. (B) A list of phosphopeptides used in the experiments. (C) A summary of phosphatase assays. Phosphopeptides from the insulin receptor were incubated with an equal amount of GST-Ptp_{rb}, GST-Ptp_{rh}, GST-Ptp_{rj} or GST-Ptp_{ro}. After the reaction, the amount of phosphate released was measured. The experiment was carried out in triplicate, and the values are shown as the mean \pm SEM.

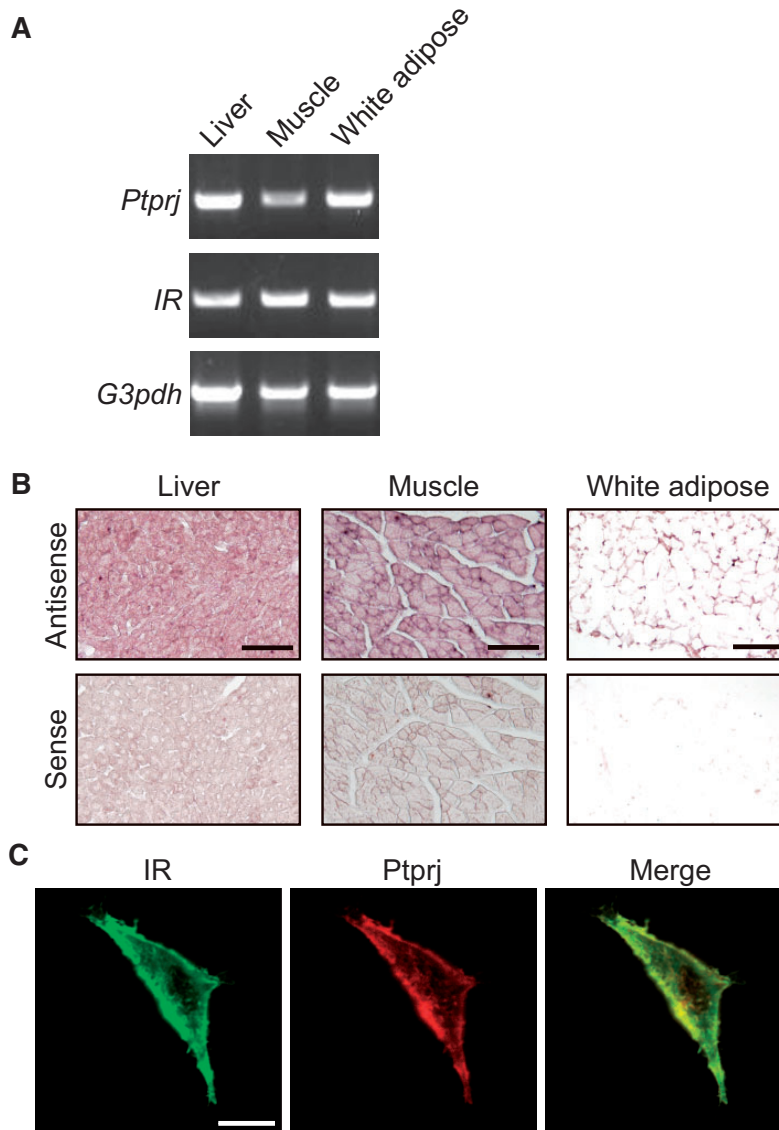


Fig. 3 Tissue and subcellular distributions of the IR and Ptp_{rj}. (A) RT-PCR analyses of *Ptp_{rj}*, *IR* and *G3pdh* gene expression in insulin target tissues. (B) Section *in situ* hybridization of *Ptp_{rj}* in insulin target tissues. Scale bars: liver, 100 μ m; muscle and white adipose, 250 μ m. (C) Subcellular distributions of the IR and Ptp_{rj} in HEK293T cells. Cells were treated with 50 ng/ml insulin for 15 min, and fixed for immunostaining. Scale bar: 10 μ m.

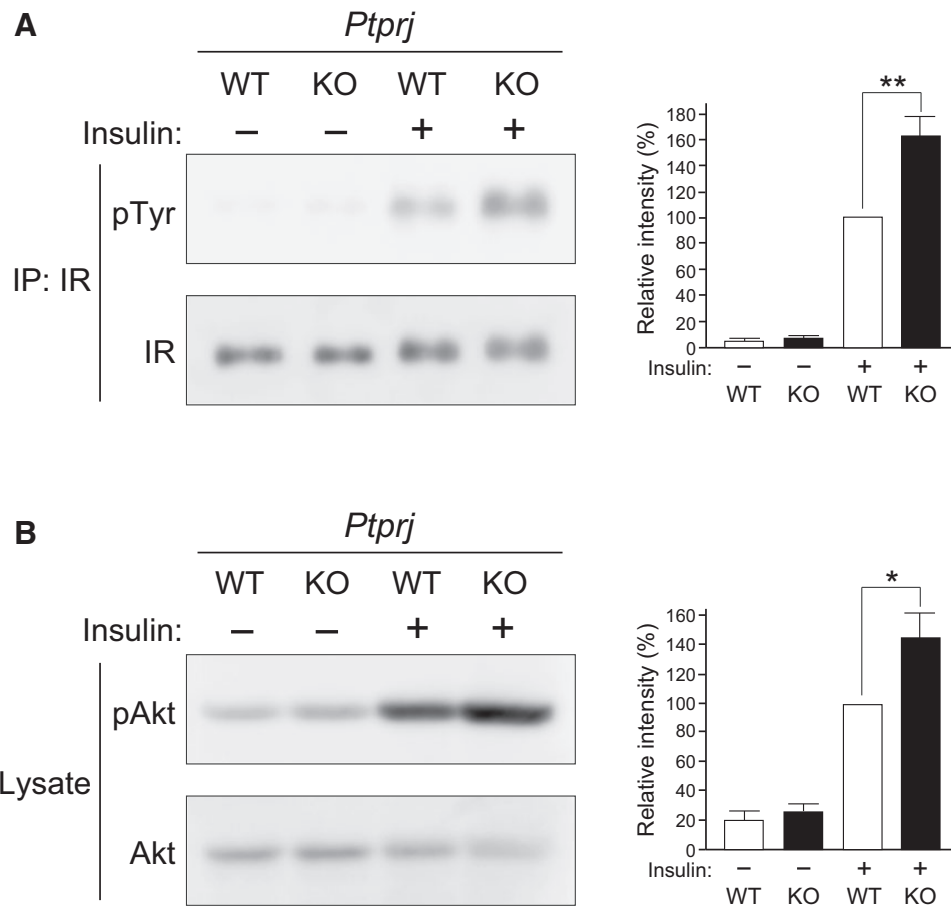


Fig. 4 Enhanced insulin signalling in the liver of *Ptprij*-KO mice. (A) Tyrosine phosphorylation levels in the IR. Mice were treated with vehicle or insulin (10 U/kg) for 5 min. IR proteins were immunoprecipitated from liver lysates with an anti-IR antibody, and subjected to immunoblotting analyses with an anti-phosphotyrosine antibody (pTyr) and anti-insulin receptor antibody (IR). The right panel shows a summary of the relative intensities of tyrosine-phosphorylated IR/IR. Data are shown as the mean \pm SEM ($n = 3$). The asterisk indicates a significant difference from WT mice by the Student's *t*-test (** $P < 0.01$). (B) Phosphorylation levels of Akt at S473. The right panel shows a summary of the relative intensities of phospho-Akt/Akt. Data are shown as the mean \pm SEM ($n = 3$). The asterisk indicates a significant difference from WT mice by the Student's *t*-test (* $P < 0.05$).

intraperitoneal injection of insulin. Prior to the administration of insulin, no significant difference was observed in the tyrosine phosphorylation levels of the IR between *Ptprij*-deficient and WT mice. However, after the insulin injection, tyrosine phosphorylation of the IR was significantly greater in *Ptprij*-KO mice than in WT mice (Fig. 4A). Furthermore, activation of the protein kinase Akt, an important downstream effector of insulin signalling, was also enhanced more in *Ptprij*-KO mice after the insulin stimulation than in WT mice (Fig. 4B). These results indicated that *Ptprij* regulated insulin signalling by dephosphorylating the IR *in vivo*.

Enhancement of glucose and insulin tolerance in *Ptprij*-KO mice

We further examined insulin sensitivity in *Ptprij*-KO mice by measuring plasma glucose concentrations after an intraperitoneal injection of glucose (glucose tolerance tests). As shown in Fig. 5A, no significant differences were observed in blood glucose concentrations between fasting *Ptprij*-KO mice and WT mice. However, as expected, *Ptprij*-KO mice cleared glucose at a higher rate than WT mice after the glucose

injection (Fig. 5A). We then performed insulin tolerance tests to confirm enhanced insulin sensitivity. After an intraperitoneal injection of insulin, the decrease observed in blood glucose levels was significantly greater in *Ptprij*-KO mice than in WT mice: an $\sim 50\%$ drop in blood glucose levels was noted in *Ptprij*-KO mice at 45 min, whereas this was $\sim 30\%$ in WT mice ($P < 0.01$) (Fig. 5B). These results strongly indicated that *Ptprij* was involved in glucose homeostasis *in vivo* by attenuating activation of the IR.

Discussion

We previously identified that the R3 RPTP subfamily specifically functioned as RPTK phosphatases for variegated RPTKs by using substrate-trapping RPTP mutants (19, 20). In this study, we additionally identified the IR as a substrate for R3 RPTPs. Substrate-trapping mutants of R3 RPTPs formed stable complexes with the IR, and more importantly, R3 RPTPs suppressed the insulin-induced tyrosine phosphorylation of the IR in cells. R3 RPTPs preferentially dephosphorylated particular phosphorylation sites in the IR: Y960 in the juxtamembrane region and

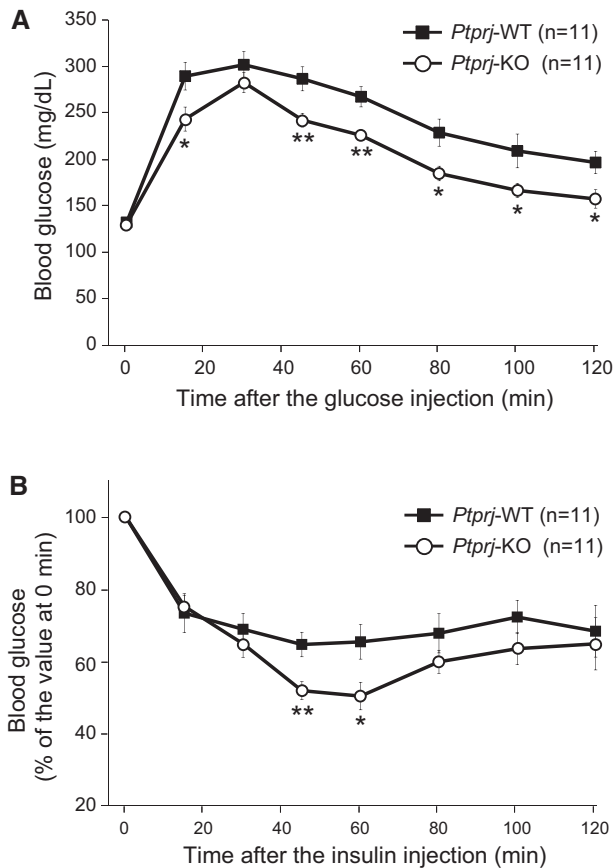


Fig. 5 Improved glucose and insulin tolerance in *Ptptrj*-KO mice. (A) Glucose tolerance test. Glucose (2 g/kg body weight) was administered by an intraperitoneal injection to fasted WT (filled squares) and *Ptptrj*-KO (open circle) mice. Blood was collected from the sectioned tip of the tail at the indicated times, and assayed for glucose using a glucometer. Values are shown as the mean \pm SEM. The asterisk indicates a significant difference from WT mice by the Student's *t*-test (* P < 0.05, ** P < 0.01). (B) Insulin tolerance test. Insulin (1 U/kg body weight) was administered by an intraperitoneal injection to fasted mice, and blood glucose levels were assayed as above. Values are shown as the mean \pm SEM. The asterisk indicates a significant difference from WT mice by the Student's *t*-test (* P < 0.05, ** P < 0.01).

Y1146 in the activation loop. Among R3 RPTPs, *Ptptrj* was selectively expressed in insulin target tissues such as the skeletal muscle, liver and adipose tissue. Furthermore, *Ptptrj* colocalized with the IR in the plasma membrane. In line with these results, *Ptptrj*-deficient mice showed enhanced insulin signalling: *Ptptrj*-deficient mice exhibited an enhancement in the insulin-induced activation of IR and Akt, and showed improved glucose and insulin tolerance. Thus, *Ptptrj* is likely to be a critical regulator of insulin signalling *in vivo*.

The binding of insulin to its receptor induces the phosphorylation of tyrosine residues in the activation loop (Y1146, Y1150 and Y1151), which leads to the full activation of tyrosine kinase (25). Following its activation, additional autophosphorylation reactions occur in the juxtamembrane region and C-terminal tail of the IR. Phosphorylation in these regions promotes interactions between signalling molecules (1). In particular, the phosphorylation of Y960 in the juxtamembrane serves as the binding site for IRS-1 and

IRS-2, which play critical roles in insulin signalling. Consequently, the activated IR induces the tyrosine phosphorylation of IRS-1 and IRS-2, which creates high-affinity binding sites for other signalling molecules, resulting in the assembly of multi-protein signalling complexes that mediate the effects of insulin on cellular metabolism, growth and glucose homeostasis (1, 2). We demonstrated that R3 RPTPs preferentially dephosphorylated Y1146 in the activation loop and Y960 in the juxtamembrane autophosphorylation sites. These results suggested that R3 RPTPs effectively inhibited IR activation and insulin signalling through the dephosphorylation of these sites. Among R3 RPTPs, *Ptptrj* was the most likely member to regulate insulin signalling *in vivo*.

PTP-1B, a ubiquitously expressed cytosolic PTP, is known to dephosphorylate the IR in order to attenuate insulin signalling *in vivo* (15, 16). *PTP1B*-deficient mice exhibit enhanced insulin sensitivity, which is associated with increased IR activation, a similar phenotype to *Ptptrj*-deficient mice. Thus, *Ptptrj* and PTP-1B may regulate insulin signalling in a similar manner *in vivo*. However, their subcellular distribution differs: *Ptptrj* is distributed in the cell membrane, whereas PTP-1B is localized at the ER via a C-terminal segment (11). Accordingly, they have different dephosphorylation site specificities in the IR: *Ptptrj* preferentially dephosphorylates Y960 and Y1146, while PTP-1B preferentially dephosphorylates Y1150/Y1151 (14). Thus, *Ptptrj* and PTP-1B appear to regulate insulin signalling via different mechanisms.

The multiple clinical manifestations of type 2 diabetes originate from defects in insulin secretion and the resistance of peripheral tissues to the effects of insulin (1). Insulin resistance has been attributed to defects in IR signalling. One approach for enhancing IR signalling may involve the inhibition of PTPs, which attenuates IR signalling *in vivo*. PTP-1B has already been recognized as a promising therapeutic target in the effective management of type 2 diabetes (30). Our results suggest that *Ptptrj* is also a promising target for the development of novel therapeutics for the treatment of type 2 diabetes and obesity. A recent study consistently showed that *Ptptrj* antisense improved the metabolic phenotype of high-fat diet-fed mice (31).

Previous studies reported that insulin entered the CNS through the blood–brain barrier by receptor-mediated transport, and regulated food intake, sympathetic activity and the effects of peripheral insulin (32, 33). Insulin signalling is also known to modulate neurotransmitter channel activity in the CNS (33). Therefore, insulin resistance in neuronal tissue may predispose individuals to the development of neurodegenerative disorders (34). Because *Ptptrj* and *Ptpro* are expressed in the CNS (26, 29), they may play an important role in the regulation of insulin signalling in the brain. The functional roles of these RPTPs in the brain need to be examined in future studies.

Insulin signalling is also involved in the normal function of endothelial cells (35): Dysfunctional insulin signalling in endothelial cells is reportedly responsible for the pathogenesis of cardiovascular impairments,

which may account for the majority of deaths in diabetic patients (35). Insulin signalling in endothelial cells also plays a pivotal role in the regulation of glucose uptake by the skeletal muscle (36). Because *Ptprb* and *Ptprj* are expressed in endothelial cells (26, 27), they may regulate insulin signalling in these cell types. Therefore, inhibitors towards these RPTPs may be potential therapeutic drugs for the cardiovascular diseases associated with diabetes and obesity. Further investigations on mice with the targeted inactivation of R3 RPTPs in different insulin target tissues may provide a definitive assessment of its contribution to IR signalling *in vivo*.

Acknowledgements

We thank Y. Dokyo and K. Wada for their technical assistance, and A. Kodama for her secretarial assistance. We thank Drs. E. Gaudio, F. Trapasso, and A. Fusco for providing us with *Ptprj* heterozygous mice.

Funding

This work was supported by grants from the Ministry of Education, Culture, Sports, Science and Technology of Japan.

Conflict of Interest

None declared.

References

- Saltiel, A.R. and Kahn, C.R. (2001) Insulin signalling and the regulation of glucose and lipid metabolism. *Nature* **414**, 799–806
- Bevan, P. (2001) Insulin signaling. *J. Cell Sci.* **114**, 1429–1430
- Drake, P.G. and Posner, B.I. (1998) Insulin receptor-associated protein tyrosine phosphatase(s): role in insulin action. *Mol. Cell. Biochem.* **182**, 79–89
- Goldstein, B.J., Ahmad, F., Ding, W., Li, P.M., and Zhang, W.R. (1998) Regulation of the insulin signalling pathway by cellular protein-tyrosine phosphatases. *Mol. Cell. Biochem.* **182**, 91–99
- Hashimoto, N., Feener, E.P., Zhang, W.R., and Goldstein, B.J. (1992) Insulin receptor protein-tyrosine phosphatases. Leukocyte common antigen-related phosphatase rapidly deactivates the insulin receptor kinase by preferential dephosphorylation of the receptor regulatory domain. *J. Biol. Chem.* **15**, 13811–13814
- Kuhné, M.R., Zhao, Z., Rowles, J., Lavan, B.E., Shen, S.H., Fischer, E.H., and Lienhard, G.E. (1994) Dephosphorylation of insulin receptor substrate 1 by the tyrosine phosphatase PTP2C. *J. Biol. Chem.* **269**, 15833–15837
- Bandyopadhyay, D., Kusari, A., Kenner, K.A., Liu, F., Chernoff, J., Gustafson, T.A., and Kusari, J. (1997) Protein-tyrosine phosphatase 1B complexes with the insulin receptor *in vivo* and is tyrosine-phosphorylated in the presence of insulin. *J. Biol. Chem.* **272**, 1639–1345
- Wälchli, S., Curchod, M.L., Gobert, R.P., Arkinstall, S., and Hooft van Huijsduijnen, R. (2000) Identification of tyrosine phosphatases that dephosphorylate the insulin receptor. A brute force approach based on “substrate-trapping” mutants. *J. Biol. Chem.* **275**, 9792–9796
- Galic, S., Klingler-Hoffmann, M., Fodero-Tavoletti, M.T., Puryer, M.A., Meng, T.C., Tonks, N.K., and Tiganis, T. (2003) Regulation of insulin receptor signaling by the protein tyrosine phosphatase TCPTP. *Mol. Cell. Biol.* **23**, 2096–2108
- Dubois, M.J., Bergeron, S., Kim, H.J., Dombrowski, L., Perreault, M., Fournès, B., Faure, R., Olivier, M., Beauchemin, N., Shulman, G.I., Siminovitch, K.A., Kim, J.K., and Marette, A. (2006) The SHP-1 protein tyrosine phosphatase negatively modulates glucose homeostasis. *Nat. Med.* **12**, 549–556
- Frangioni, J.V., Beahm, P.H., Shifrin, V., Jost, C.A., and Neel, B.G. (1992) The nontransmembrane tyrosine phosphatase PTP-1B localizes to the endoplasmic reticulum via its 35 amino acid C-terminal sequence. *Cell* **68**, 545–560
- Norris, K., Norris, F., Kono, D.H., Vestergaard, H., Pedersen, O., Theofilopoulos, A.N., and Møller, N.P. (1997) Expression of protein-tyrosine phosphatases in the major insulin target tissues. *FEBS Lett.* **415**, 243–248
- Bourdeau, A., Dubé, N., and Tremblay, M.L. (2005) Cytoplasmic protein tyrosine phosphatases, regulation and function: the roles of PTP1B and TC-PTP. *Curr. Opin. Cell Biol.* **17**, 203–209
- Salmeen, A., Andersen, J.N., Myers, M.P., Tonks, N.K., and Barford, D. (2000) Molecular basis for the dephosphorylation of the activation segment of the insulin receptor by protein tyrosine phosphatase 1B. *Mol. Cell* **6**, 1401–1412
- Elchebly, M., Payette, P., Michaliszyn, E., Cromlish, W., Collins, S., Loy, A.L., Normandin, D., Cheng, A., Himms-Hagen, J., Chan, C.C., Ramachandran, C., Gresser, M.J., Tremblay, M.L., and Kennedy, B.P. (1999) Increased insulin sensitivity and obesity resistance in mice lacking the protein tyrosine phosphatase-1B gene. *Science* **283**, 1544–1548
- Klaman, L.D., Boss, O., Peroni, O.D., Kim, J.K., Martino, J.L., Zabolotny, J.M., Moghal, N., Lubkin, M., Kim, Y.B., Sharpe, A.H., Stricker-Krongrad, A., Shulman, G.I., Neel, B.G., and Kahn, B.B. (2000) Increased energy expenditure, decreased adiposity, and tissue-specific insulin sensitivity in protein-tyrosine phosphatase 1B-deficient mice. *Mol. Cell. Biol.* **20**, 5479–5489
- Alonso, A., Sasin, J., Bottini, N., Friedberg, I., Friedberg, I., Osterman, A., Godzik, A., Hunter, T., Dixon, J., and Mustelin, T. (2004) Protein tyrosine phosphatases in the human genome. *Cell* **117**, 699–711
- Andersen, J.N., Jansen, P.G., Echwald, S.M., Mortensen, O.H., Fukada, T., Del Vecchio, R., Tonks, N.K., and Møller, N.P. (2004) A genomic perspective on protein tyrosine phosphatases: gene structure, pseudogenes, and genetic disease linkage. *FASEB J.* **18**, 8–30
- Sakuraba, J., Shintani, T., Tani, S., and Noda, M. (2013) Substrate specificity of R3 receptor-like protein-tyrosine phosphatase subfamily toward receptor protein-tyrosine kinases. *J. Biol. Chem.* **288**, 23421–23431
- Shintani, T., Ihara, M., Sakuta, H., Takahashi, H., Watakabe, I., and Noda, M. (2006) Eph receptors are negatively controlled by protein tyrosine phosphatase receptor type O. *Nat. Neurosci.* **9**, 761–769
- Shintani, T., Ihara, M., Tani, S., Sakuraba, J., Sakuta, H., and Noda, M. (2009) APC2 plays an essential role in axonal projections through the regulation of microtubule stability. *J. Neurosci.* **29**, 11628–11640
- Trapasso, F., Drusco, A., Costinean, S., Alder, H., Aqeilan, R.I., Iuliano, R., Gaudio, E., Raso, C., Zanesi, N., Croce, C.M., and Fusco, A. (2006) Genetic ablation of *Ptprj*, a mouse cancer susceptibility gene,

- results in normal growth and development and does not predispose to spontaneous tumorigenesis. *DNA Cell Biol.* **25**, 376–382
23. Flint, A.J., Tiganis, T., Barford, D., and Tonks, N.K. (1997) Development of “substrate-trapping” mutants to identify physiological substrates of protein tyrosine phosphatases. *Proc. Natl. Acad. Sci. U S A.* **94**, 1680–1685
 24. Ottensmeyer, F.P., Beniac, D.R., Luo, R.Z., and Yip, C.C. (2000) Mechanism of transmembrane signaling: insulin binding and the insulin receptor. *Biochemistry* **39**, 12103–12112
 25. White, M.F., Shoelson, S.E., Keutmann, H., and Kahn, C.R. (1998) A cascade of tyrosine autophosphorylation in the beta-subunit activates the phosphotransferase of the insulin receptor. *J. Biol. Chem.* **263**, 2969–2980
 26. Gaya, A., Piroto, F., Palou, E., Autschbach, F., Del Pozo, V., Sole, J., and Serra-Pages, C. (1999) CD148, a new membrane tyrosine phosphatase involved in leukocyte function. *Leuk. Lymphoma* **35**, 237–243
 27. Fachinger, G., Deutsch, U., and Risau, W. (1999) Functional interaction of vascular endothelial-protein-tyrosine phosphatase with the angiopoietin receptor Tie-2. *Oncogene* **18**, 5948–5953
 28. Sadakata, H., Okazawa, H., Sato, T., Supriatna, Y., Ohnishi, H., Kusakari, S., Murata, Y., Ito, T., Nishiyama, U., Minegishi, T., Harada, A., and Matozaki, T. (2009) SAP-1 is a microvillus-specific protein tyrosine phosphatase that modulates intestinal tumorigenesis. *Genes Cells* **14**, 295–308
 29. Beltran, P.J., Bixby, J.L., and Masters, B.A. (2003) Expression of PTPRO during mouse development suggests involvement in axonogenesis and differentiation of NT-3 and NGF-dependent neurons. *J. Comp. Neurol.* **456**, 384–395
 30. Barr, A.J. (2010) Protein tyrosine phosphatases as drug targets: strategies and challenges of inhibitor development. *Future Med. Chem.* **2**, 1563–1576
 31. Krüger, J., Trappiel, M., Dagnell, M., Stawowy, P., Meyborg, H., Böhm, C., Bhanot, S., Ostman, A., Kintscher, U., and Kappert, K. (2013) Targeting density-enhanced phosphatase-1 (DEP-1) with antisense oligonucleotides improves the metabolic phenotype in high-fat diet-fed mice. *Cell Commun. Signal.* **11**, 49
 32. Brüning, J.C., Gautam, D., Burks, D.J., Gillette, J., Schubert, M., Orban, P.C., Klein, R., Krone, W., Müller-Wieland, D., and Kahn, C.R. (2000) Role of brain insulin receptor in control of body weight and reproduction. *Science* **289**, 2122–2125
 33. Kleinridders, A., Ferris, H.A., Cai, W., and Kahn, C.R. (2014) Insulin action in brain regulates systemic metabolism and brain function. *Diabetes* **63**, 2232–2243
 34. Schubert, M., Gautam, D., Surjo, D., Ueki, K., Baudler, S., Schubert, D., Kondo, T., Alber, J., Galldiks, N., Küstermann, E., Arndt, S., Jacobs, A.H., Krone, W., Kahn, C.R., and Brüning J.C. (2004) Role for neuronal insulin resistance in neurodegenerative diseases. *Proc. Natl. Acad. Sci. U S A.* **101**, 3100–3105
 35. Manrique, C., Lastra, G., and Sowers, J.R. (2014) New insights into insulin action and resistance in the vasculature. *Ann. N Y Acad. Sci.* **1311**, 138–1350
 36. Kubota, T., Kubota, N., and Kadowaki, T. (2013) The role of endothelial insulin signaling in the regulation of glucose metabolism. *Rev. Endocr. Metab. Disord.* **14**, 207–216